

Giant amplification of noise in fluctuation-induced pattern formation

Tommaso Biancalani,* Farshid Jafarpour,† and Nigel Goldenfeld

Department of Physics, University of Illinois at Urbana-Champaign,
Loomis Laboratory of Physics, 1110 West Green Street, Urbana, Illinois, 61801-3080. and
Carl R. Woese Institute for Genomic Biology, University of Illinois at Urbana-Champaign,
1206 West Gregory Drive, Urbana, Illinois 61801.

(Dated: June 16, 2016)

The amplitude of fluctuation-induced patterns might be expected to be proportional to the strength of the driving noise, suggesting that such patterns would be difficult to observe in nature. Here, we show that a large class of spatially-extended dynamical systems driven by intrinsic noise can exhibit giant amplification, yielding patterns whose amplitude is comparable to that of deterministic Turing instabilities. The giant amplification results from the interplay between noise and non-orthogonal eigenvectors of the linear stability matrix, yielding transients that grow with time, and which, when driven by the ever-present intrinsic noise, lead to persistent large amplitude patterns. This mechanism provides a robust basis for fluctuation-induced biological pattern formation based on the Turing mechanism, without requiring fine tuning of diffusion constants.

Since the seminal paper of Turing [1], it has been recognized that pattern forming dynamical instabilities could potentially underlie various examples of biological pattern formation and development [2]. The Turing mechanism has two major assumptions: first, that two chemical species behave as an activator-inhibitor system (but see a recent extension [3]), and secondly, that the spatial diffusion constant of the inhibitor is greater than that of the activator, typically by two orders of magnitude or more [4]. However, this second condition is not generally present in experimental observations [5, 6]. The widely-held conclusion is that biological patterns reflect gene expression and the interplay of developmental processes, so that the Turing mechanism itself is not generally operative [7].

This conclusion relies upon a third assumption of Turing patterns: that they are deterministic. However, many biological systems exhibit strong fluctuations due to demographic stochasticity, arising from (e.g.) finite population size (ecology) or copy number (gene expression), and these fluctuations could potentially couple to the underlying pattern-forming instabilities. Detailed analysis shows that the length scale of fluctuation-induced patterns is set by the same condition as in the deterministic Turing analysis, but remarkably the pattern exists over a wide range of parameter values, even where the diffusion constants of activator and inhibitor are of similar magnitudes [8–13]. These fluctuation-induced or stochastic patterns arise physically because, even though the uniform unpatterned state is linearly stable, the demographic fluctuations are constantly pushing the system slightly away from its stable fixed point; if the resulting small amplitude dynamics is dominated by an eigenvalue with a non-zero wavelength, then a spatial pattern can arise.

This mechanism suggests that the amplitude of fluctuation-induced patterns would be set by $\Omega^{-1/2}$, where Ω indicates the population size within a correlation

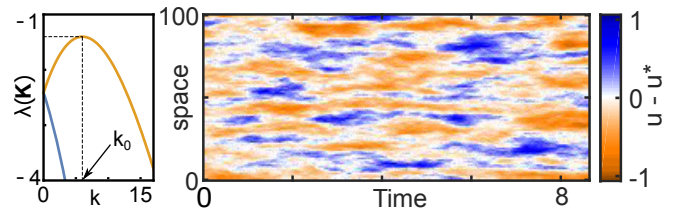


FIG. 1. (Color online) **Turing-like pattern with large amplitude and comparable diffusivities.** (right panel) Stochastic simulations [14] of a two-species model (12) with diffusivities $\delta_U = 3.9$, $\delta_V = 3.4\delta_U$ and system size $\Omega = 10^4$. Patterns are noise-induced as they arise from a stable homogeneous state u^* , *i.e.*, the eigenvalues λ plotted against the wavelength k are negative (left panel). However, the pattern amplitude results of the order of one (right bar). Other parameters: $a = 3$, $b = 5.8$, $c = e = 1$.

volume of the system, *ie.* the spatial patch within which the system can be considered to be well mixed [8, 9]. Thus in situations where $\Omega \gg 1$, fluctuation-induced patterns might have a very small amplitude compared to deterministic Turing patterns, potentially diminishing their relevance for biological and ecological pattern formation.

The purpose of this Letter is to show that fluctuation-induced Turing patterns can readily be observed, even when the noise is very small and the ratio of diffusion constants is close to one. Specifically we present an analytical theory showing the presence of giant amplification, due to an interplay between a separation of time scales and non-normality of the eigenvectors in the linear stability analysis about a uniform stable steady state. We present a measure of non-normality for a general stochastic dynamical system near a stable fixed point, with a clear geometrical interpretation. We then show that giant amplification occurs in a wide class of fluctuation-induced pattern-forming systems. An example of our key result described below is shown in Fig. 1: stochastic simulations of the generic pattern-forming model of Ridolfi et

al. [15], performed on a linear chain of 10^2 spatial cells, each cell with a system size of $\Omega = 10^4$. Patterns are noise-induced as they arise from a stable homogeneous state (left panel), but despite the factor $\Omega^{-1/2} = 10^{-2}$ the resulting amplitude is of order unity.

This giant amplification is due to the counterintuitive fact that the dynamics following a small displacement from a stable fixed point need not relax back to the fixed point monotonically: there can be an initial transient amplification if the linear stability matrix is non-normal: that is, it does not admit an orthogonal set of eigenvectors (Fig. 2). Non-normality has been thoroughly investigated, at a deterministic level, in fluid dynamics [16, 17], and in ecology [18, 19], and is a common feature of pattern-forming systems [15, 20]. Low-dimensional stochastic non-normal systems may also exhibit strong amplification of noise [21]. The specific contribution of the present paper is to systematically analyze the role of non-normality in fluctuation-induced spatial patterns, and to show that its widespread occurrence suggests a new way in which fluctuation-induced Turing patterns may play a wider role in biological and ecological pattern formation than previously recognized.

Non-normality in stochastic dynamics:- We begin by introducing a measure to quantify the degree of amplification in a well-mixed stochastic system. Consider the linear stochastic differential equation for an m -component state vector \vec{y} :

$$\dot{\vec{y}} = \mathbf{A}\vec{y} + \sigma \vec{\eta}(t), \quad (1)$$

where the components of $\vec{\eta}$, are normalized Gaussian white noises and the model-dependent matrix \mathbf{A} has negative real eigenvalues, λ_i ($i = 1, \dots, m$). Therefore, the fixed point $\vec{y}_0 = 0$ is stable. The coefficient σ represents the strength of the fluctuations and scales with the system size $\Omega^{-1/2}$ in the case of demographic noise. Equation (1) is the prototypical linearization of stochastic dynamics near a stable fixed point, and we analyze the mean square displacement from the fixed point, $\langle \|\vec{y}\|^2 \rangle$, where $\|\vec{y}\| = \sqrt{\vec{y}^T \vec{y}}$, is the Euclidean norm.

Since all the eigenvalues of \mathbf{A} are negative, under the deterministic part of Eq. (1), all the components of \vec{y} decay exponentially to zero along the eigenvectors of \mathbf{A} , with decay time scales $\tau_i = \lambda_i^{-1}$. In contrast, the noise term provides stochastic agitation with a strength proportional to σ . One might intuitively expect that an upper bound for $\langle \|\vec{y}\|^2 \rangle$ could be found by replacing all the eigenvalues by the eigenvalues corresponding to the slowest decaying mode, $\lambda = \max\{\lambda_i\}$. Therefore, the norm of \vec{y}_u with the dynamics $\dot{\vec{y}}_u = \lambda \vec{y}_u + \sigma \vec{\eta}(t)$, should provide an upper bound for $\|\vec{y}\|$. The mean square norm

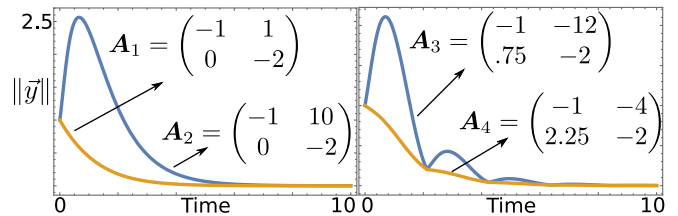


FIG. 2. (Color online) **Stable linear systems can amplify perturbations [18]**. Dynamics of the Euclidean norm $\|\vec{y}\|$ obtained by solving $\dot{\vec{y}} = \mathbf{A}_i \vec{y}$. Reactive systems exhibit transient amplification before relaxing to fixed point (blue lines), in contrast with conventional response of stable systems (yellow lines). Matrices \mathbf{A}_1 and \mathbf{A}_2 (respectively \mathbf{A}_3 and \mathbf{A}_4) have same real (respectively complex conjugate) eigenvalues.

of \vec{y}_u is given by ($\tau = -\lambda^{-1}$):

$$\langle \|\vec{y}_u\|^2 \rangle = \left\langle \left\| \int_0^{\tau/2} \vec{\eta}(t) dt \right\|^2 \right\rangle = \frac{m}{2} \tau \sigma^2. \quad (2)$$

However, this upper bound is only valid when the matrix \mathbf{A} is normal, *i.e.* it has an orthogonal set of eigenvectors (for instance, Hermitian matrices are normal) [21]. This can be understood by analyzing the behavior of Eq. (1) in the deterministic limit ($\sigma = 0$). Although the asymptotic decay rate of $\|\vec{y}\|$ is set by the eigenvalues of \mathbf{A} , the instantaneous response is given by the eigenvalues of $\mathbf{H} = (\mathbf{A} + \mathbf{A}^T)/2$, the Hermitian part of \mathbf{A} [18]. If \mathbf{A} is non-normal, then the short-time dynamics of $\|\vec{y}\|$ cannot be predicted by the eigenvalues of \mathbf{A} . Remarkably, \mathbf{H} can admit positive eigenvalues even though \mathbf{A} possesses all negative eigenvalues, in which case $\|\vec{y}\|$ can experience a transient growth, for suitable initial conditions, before it starts decaying (Fig. 2). This mechanism, sometimes termed as reactivity [18], occurs because the transformation that takes \vec{y} to the eigenbasis of \mathbf{A} is not unitary if the eigenvectors of \mathbf{A} are not orthogonal, and thus does not preserve the norm of \vec{y} . Clearly, if the stable matrix amplifies perturbations, the bound (2) cannot hold.

In the presence of noise, this transient effect in the deterministic part of Eq. (1) has a lasting effect on the steady state amplitude of the stochastic dynamics. This can be demonstrated by solving the steady state probability density of \vec{y} for Eq. (1). The detailed derivation of what follows is presented in the supplemental material (SM). For every stable matrix \mathbf{A} , we define a matrix \mathbf{G} such that the Hermitian part of its inverse is the identity, and its product with \mathbf{A} is Hermitian, that is,

$$\frac{1}{2} \left(\mathbf{G}^{-1} + (\mathbf{G}^{-1})^T \right) = \mathbb{1}, \quad (\mathbf{G}\mathbf{A})^T = \mathbf{G}\mathbf{A}. \quad (3)$$

Note that \mathbf{G} is the identity matrix if \mathbf{A} is Hermitian. In terms of this matrix \mathbf{G} , the steady state probability

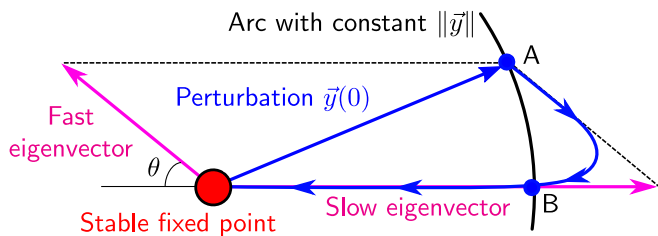


FIG. 3. (Color online) **Transient amplification is caused by non-orthogonal eigenvectors and a separation of timescales.** The stable fixed point is subject to the perturbation $\vec{y}(0)$. Because of the separation of timescales, the deterministic trajectory (blue arrowed line) is initially parallel to the fast eigenvector before relaxing to the slow manifold. From A to B, the trajectory has magnitude greater than $\|\vec{y}_0\|$.

density of \vec{y} is given by

$$P(\vec{y}) = \sqrt{\det\left(-\frac{\mathbf{GA}}{\pi\sigma^2}\right)} \exp\left(-\frac{\vec{y}^T \mathbf{GA} \vec{y}}{\sigma^2}\right), \quad (4)$$

hence the mean square value of $\|\vec{y}\|$ is (tr stands for the trace function)

$$\langle \|\vec{y}\|^2 \rangle = -\frac{\sigma^2}{2} \mathcal{H}(\mathbf{A}) \text{tr}(\mathbf{A}^{-1}), \quad (5)$$

where we have defined the non-normality index \mathcal{H} by:

$$\mathcal{H}(\mathbf{A}) = \text{tr}(\mathbf{G}^{-1} \mathbf{A}^{-1}) / \text{tr}(\mathbf{A}^{-1}). \quad (6)$$

Note that we always have $\mathcal{H} \geq 1$, and \mathcal{H} is equal to one if and only if the matrix \mathbf{A} is normal. Moreover, the further \mathbf{A} is from normal, the larger is the index \mathcal{H} . In the case of a two-dimensional matrix \mathbf{A} , the non-normality index \mathcal{H} simplifies to the following simple expression, where $\cot\theta$ is the cotangent of the angle between the two eigenvectors:

$$\mathcal{H} = 1 + \cot^2(\theta) \left(\frac{\lambda_1 - \lambda_2}{\lambda_1 + \lambda_2} \right)^2. \quad (7)$$

This expression gives us quantitative understanding about how transient amplification occurs (Fig. 3). Two ingredients are necessary: non-orthogonal eigenvectors and a separation of time scales given by eigenvalues of different magnitudes. If the system is not subject to noise, suitable initial conditions are also required (e.g. the blue vector in Fig. 3). Because of the separation of time scales, the component of \vec{y} along the eigenvector associated with the faster eigenvalue decays quickly, whereas in the slow direction the dynamics is approximately constant. However, because of non-orthogonality, the norm of \vec{y} instantaneously increases as \vec{y} moves along the fast eigenvector, until the slow manifold starts attracting the trajectory back to fixed point.

Non-normality in spatially-extended pattern formation:- We now analyze spatially-extended, diffusively-coupled pattern-forming systems driven by noise. Specifically, we consider the generic equation

$$\frac{\partial \vec{q}}{\partial t} = \vec{f}(\vec{q}) + \mathbf{D} \nabla^2 \vec{q} + \sigma \vec{\xi}(\vec{x}, t), \quad (8)$$

where \vec{x} is a space variable, the vector $\vec{q} = (q_1, q_2)$, the diffusion matrix $\mathbf{D} = \text{diag}(D_1, D_2)$, and ξ_i 's, the components of $\vec{\xi}(\vec{x}, t)$ are normalized δ -correlated Gaussian white noises. Also, we assume that $\vec{f}(\vec{q})$ has a stable fixed point \vec{q}^* , and all of the eigenvalues of the linear stability or Jacobian matrix $\mathbf{J} = \nabla_{\vec{q}} f(\vec{q})|_{\vec{q}^*}$ have negative real part.

Our goal is to show that in the presence of noise, system (8) exhibits patterns in a parameter regime where the fixed point \vec{q}^* is stable. The stability of \vec{q}^* can be inspected by defining the deviation $\vec{p} = \vec{q} - \vec{q}^*$ and linearizing near \vec{q}^* , yielding

$$\frac{\partial \vec{p}}{\partial t} = \mathbf{J} \vec{p} + \mathbf{D} \nabla^2 \vec{p} + \sigma \vec{\xi}(\vec{x}, t). \quad (9)$$

The spatial degrees of freedom can be diagonalized by a Fourier transform ($\vec{x} \mapsto \vec{k}$), resulting in

$$\frac{d\vec{p}_{\vec{k}}}{dt} = \mathbf{K} \vec{p}_{\vec{k}} + \sigma \vec{\xi}(\vec{k}, t), \quad \mathbf{K} = \mathbf{J} - k^2 \mathbf{D}. \quad (10)$$

The equations are now decoupled and are therefore tantamount to Eq. (1).

We start by reviewing the stability of the deterministic part of Eq. (9). If $D_1 = D_2$, matrix \mathbf{D} is a multiple of the identity, and the eigenvalues of \mathbf{K} will be the eigenvalues of \mathbf{J} shifted by $-k^2 D$ for each \vec{k} , resulting in a more stable operator. However, in the case that the diffusion rates are sufficiently different, the largest eigenvalue of \mathbf{K} can have a non-monotonic behavior as a function of \vec{k} , and in some cases have positive eigenvalues for a small range of \vec{k} peaked around some non-zero value \vec{k}_0 . In this case, the modes near \vec{k}_0 will grow leading to the formation of deterministic Turing patterns [1]. Therefore, the formation of deterministic Turing patterns is dependent on a large separation of the diffusion constants [4–6].

In contrast, consider an intermediate scenario with diffusion constants different enough so that they can cause a non-monotonic behavior for the largest eigenvalue of \mathbf{K} as a function of \vec{k} peaked around some value \vec{k}_0 , but not enough for the largest eigenvalue to become positive at any k (left panel of Fig. 1). In this case, all the \vec{k} modes decay quickly to zero, but the modes with $\vec{k} \sim \vec{k}_0$ decay slower than the others, causing a transient pattern. In the presence of the noise term $\vec{\xi}(\vec{k}, t)$ in Eq. (10), while the modes with smaller eigenvalues decay quickly to zero, the slow modes drift away from the fixed point under the influence of the noise. The drift of the \vec{k} modes near \vec{k}_0 produces persistent steady-state fluctuation-induced

patterns with well-defined length-scales [8, 9]. While the stochastic Turing patterns have a less stringent requirement than the deterministic Turing patterns for the ratio of the diffusion constants, their amplitude is limited to the amplitude of the drift under the noise suppressed by the slow deterministic decay. As discussed in the previous section, the mean square amplitude is of order $\lambda^{-1}\sigma^2$, unless we can show that the system is non-normal.

We now prove that in order for a system described by Eq. (8) to produce stochastic patterns, it is necessary for the matrix \mathbf{J} in Eq. (9) to be non-normal. We show this by finding a lower bound on the difference between the largest eigenvalue of $\mathbf{H} = (\mathbf{J} + \mathbf{J}^T)/2$ and that of matrix \mathbf{J} . The proof relies on the fact that for the system to exhibit stochastic patterns, the real part of the largest eigenvalue, λ_1 , of \mathbf{K} as a function of the wave vector \vec{k} should peak at some value $\vec{k}_0 \neq 0$ [9, 22], and therefore, $\delta = \Re(\lambda_1(\mathbf{K}_0)) - \Re(\lambda_1(\mathbf{J})) > 0$, for $\mathbf{K}_0 = \mathbf{K}(\vec{k}_0)$. It is a well known fact that the real part of the largest eigenvalue of a matrix is less than or equal to that of its Hermitian part (*e.g.* see Ref. [23]), therefore, $\Re(\lambda_1(\mathbf{K}_0)) \leq \lambda_1(\mathbf{H} - k_0^2 \mathbf{D})$. Since both \mathbf{H} and $-k_0^2 \mathbf{D}$ are Hermitian, by Weyl inequality $\lambda_1(\mathbf{H} - k_0^2 \mathbf{D}) \leq \lambda_1(\mathbf{H}) + \lambda_1(-k_0^2 \mathbf{D}) = \lambda_1(\mathbf{H}) - k_0^2 D_{min}$. Adding $k_0^2 D_{min} - \Re(\lambda_1(\mathbf{J}))$ to both sides of this inequality, we arrive at

$$\lambda_1(\mathbf{H}) - \Re(\lambda_1(\mathbf{J})) \geq \delta + k_0^2 D_{min}. \quad (11)$$

Since the non-normality of \mathbf{J} should be independent of the diffusion constants, this lower bound can be extended to the supremum of the right hand side of the inequality (11) over all the matrices \mathbf{D} that produce spatial patterns and their corresponding \vec{k}_0 . In particular, if a system admits deterministic Turing patterns for some set of diffusion constants, *i.e.* $\Re(\lambda_1(\mathbf{K}_0)) > 0$, δ would be greater than $-\Re(\lambda_1(\mathbf{J}))$, and therefore \mathbf{J} would be reactive (this special case was previously proven by Neubert et al. [20]). In this case, if experimentally measured values of diffusion constants do not fall within the Turing pattern regime, the system is still reactive and capable of exhibiting amplified stochastic patterns.

Stochastic extension of model by Ridolfi et al. :- Finally, we apply our theory to a concrete model that is representative of a large class of systems. On a deterministic level, the model is given by Eq. (8) with two species U and V with densities $\vec{q} = (u, v)$, and $\vec{f}(u, v) = (u(a uv - e), v(b - cu^2 v))$, with $a, b, c, e > 0$ [15]. The corresponding stochastic model is defined by considering the following individual-level processes that occur on a discretized D -dimensional space with L^D lattice sites,

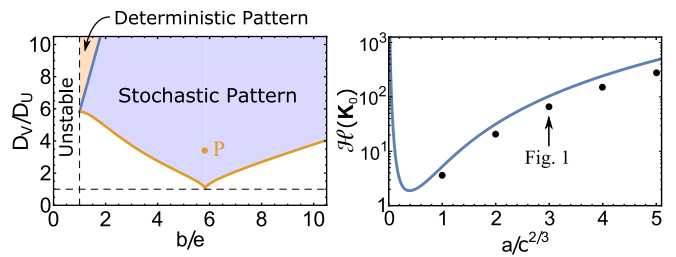
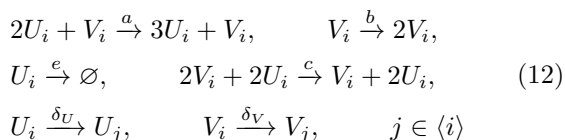


FIG. 4. (Color online) **Stochasticity allows pattern formation for similar diffusivities.** (left) Phase diagram of model (12) showing that the pattern forming behavior of this model depends only on the ratios b/a and D_V/D_U (see SM for analytic expression for the boundaries). (right) Semi-log plot of non-normality index for the point P as a function of $a/c^{2/3}$. Black markers are amplifications measured in simulation.

where U_i and V_i are the species U and V on the site i for $i = 1 \dots L^D$ and $\langle i \rangle$ is the set of sites neighboring i . The state of the system is specified by the concentration vectors $\vec{q}_i \equiv (u_i, v_i) \equiv (U_i, V_i)/\Omega$, where Ω is the volume of each site. The diffusion rates δ_u and δ_v are related to the diffusion constants by $(\delta_u, \delta_v) = (D_U, D_V)/\Omega^{2/D}$. The discrete-space version of Eqs. (8), (9) and (10) are derived by expanding in powers of $\Omega^{-1/2}$ the master equation corresponding to scheme (12) (see the SM for the derivations).

The pattern forming behavior of the model described by (12) only depends on the ratio of the diffusion constants D_V/D_U and the ratio of the reaction rates of the two linear reactions b/e . The left panel of Figure 4 shows the regime of parameters in which the system exhibits either stochastic or deterministic Turing patterns. As expected, deterministic patterns emerge only when the ratio D_V/D_U of diffusion constants is very large (above the blue line in Fig. 4 which steeply grows outside of the figure), while the requirement on this ratio for the stochastic patterns is drastically reduced (see the SM for analytic expressions for the boundaries). In the absence of the non-normality effect, one would expect that only stochastic patterns with parameters very close to the deterministic regime would be observed, since far from this regime, the amplitude of the patterns would be too small to detect.

However, since for all $b/e > 1$, there is a D_V/D_U above which the system exhibits deterministic Turing patterns, \mathbf{J} is reactive. Therefore, even when the system is far from the parameter regime of deterministic patterns, the amplitude of the stochastic patterns is far larger than what one would expect from the analysis of the eigenvalues from Eq. (2). We can see this by analyzing the amplitude of the patterns at the point P in Fig. 4. This point has ratios $b/e = 5.8$ and $D_V/D_U = 3.4$ and is chosen to be very far from the deterministic Turing pattern regime. At this b/e ratio, the ratio of the diffusion constants has to be at least ten times larger than the chosen

value for the system to exhibit deterministic Turing patterns. The amplitude of the patterns as determined by Eq. (5) is dependent on the eigenvalues of \mathbf{K} (fixed by the choice of the point P) and the non-normality index $\mathcal{H}(\mathbf{K})$ which can be tuned by changing the ratio $a/c^{2/3}$ without changing the point P (see SM for the analytic expression). The right panel of Figure 4 shows that the amplification of stochastic patterns for the point P varies over orders of magnitude for a small range of $a/c^{2/3}$.

The right panel of Figure 2 shows the time series of the amplified stochastic Turing patterns in the concentration of the species U , in a simulation of our model in one dimension. The mean square amplitude of these spatial patterns is about 0.21, while the upper bound for the amplitude of the pattern in the absence of reactivity from Eq. (2) is 2.5×10^{-3} . The non-normality index \mathcal{H} of the slowest Fourier mode $k_0 = 6$ is about 103 justifying the two order of magnitude amplification in the amplitude of the stochastic patterns (see the right panel of Fig. 4).

In conclusion, fluctuation-induced Turing patterns have larger amplitude than previously expected, even when the ratio of the diffusion coefficients is far from the requirement for deterministic Turing patterns. This large amplitude is due to non-normality of the type of interactions that are required for a system to produce Turing-like patterns. We have introduced a new measure of non-normality that is applicable to all stochastic dynamical systems and measures the amplification of the expected value of the distance that a non-equilibrium system maintains from its fixed point at steady state. We have used this measure to quantify the effect of non-normality on stochastic Turing patterns and explain the unexpectedly large amplitude observed in the simulations. By analyzing an example of an activator-inhibitor system, we have shown that the demographic stochasticity drastically expands the range of parameters in which the system exhibits Turing-like patterns, and that these patterns have amplitudes that are orders of magnitude larger than expected in all but a narrow region in parameter space. We conclude that fluctuation-induced Turing patterns can readily be observed, and therefore, provide a potential mechanism explaining a wide range of pattern formations observed in ecology, biology, and development

This work was supported by the National Aeronautics and Space Administration Astrobiology Institute (NAI) under Cooperative Agreement No. NNA13AA91A issued through the Science Mission Directorate. T.B acknowledges partial funding from the National Science Foundation under Grant No. PHY-105515. T. B. and F. J. Contributed equally to this work.

* Present address: Physics of Living Systems, Department of Physics, Massachusetts Institute of Technology, Cambridge, MA

† T. Biancalani and F. Jafarpour contributed equally to this work.

- [1] A. M. Turing, Philos. Trans. R. Soc. London, Ser. B **237**, 37 (1952).
- [2] A. Koch and H. Meinhardt, Rev. Mod. Phys. **66**, 1481 (1994).
- [3] S. Werner, T. Stückemann, M. B. Amigo, J. C. Rink, F. Jülicher, and B. M. Friedrich, Phys. Rev. Lett. **114**, 138101 (2015).
- [4] J. D. Murray, *Mathematical Biology. II Spatial Models and Biomedical Applications {Interdisciplinary Applied Mathematics V. 18}* (Springer-Verlag New York Incorporated, 2001).
- [5] V. Castets, E. Dulos, J. Boissonade, and P. De Kepper, Phys. Rev. Lett. **64**, 2953 (1990).
- [6] Q. Ouyang and H. L. Swinney, Nature **352**, 610 (1991).
- [7] P. K. Maini, T. E. Woolley, R. E. Baker, E. A. Gaffney, and S. S. Lee, Interface focus, rsfs20110113 (2012).
- [8] T. Butler and N. Goldenfeld, Phys. Rev. E **80**, 030902 (2009).
- [9] T. Biancalani, D. Fanelli, and F. Di Patti, Phys. Rev. E **81**, 046215 (2010).
- [10] S. Datta, G. W. Delius, R. Law, and M. J. Plank, J. Math. Bio. **63**, 779 (2011).
- [11] L. Ridolfi, P. D'Odorico, and F. Laio, *Noise-Induced Phenomena in the Environmental Sciences* (Cambridge University Press, Cambridge, 2011).
- [12] J. A. Bonachela, M. A. Muñoz, and S. A. Levin, J. Stat. Phys. **148**, 724 (2012).
- [13] T. C. Butler, M. Benayoun, E. Wallace, W. van Drongele, N. Goldenfeld, and J. Cowan, Proc. Natl. Acad. Sci. USA **109**, 606 (2012).
- [14] D. T. Gillespie, A. Hellander, and L. R. Petzold, J. Chem. Phys. **138**, 170901 (2013).
- [15] L. Ridolfi, C. Camporeale, P. D'Odorico, and F. Laio, Eur. Phys. Lett. **95**, 18003 (2011).
- [16] L. Trefethen, A. Trefethen, S. Reddy, T. Driscoll, *et al.*, Science **261**, 578 (1993).
- [17] L. N. Trefethen and M. Embree, *Spectra and pseudospectra: the behavior of nonnormal matrices and operators* (Princeton University Press, 2005).
- [18] M. G. Neubert and H. Caswell, Ecology **78**, 653 (1997).
- [19] S. Tang and S. Allesina, Population Dynamics **2**, 21 (2014).
- [20] M. G. Neubert, H. Caswell, and J. Murray, Mathematical biosciences **175**, 1 (2002).
- [21] B. F. Farrell and P. J. Ioannou, Phys. Rev. Lett. **72**, 1188 (1994).
- [22] A. J. McKane, T. Biancalani, and T. Rogers, Bull. Math. Biol. **76**, 895 (2014).
- [23] M. Adam and M. J. Tsatsomeros, Electron. J. Linear Algebra **15**, 239 (2006).
- [24] C. W. Gardiner, *Handbook of Stochastic Methods for Physics, Chemistry and the Natural Sciences*, 4th ed. (Springer, New York, 2009).
- [25] N. G. van Kampen, *Stochastic Processes in Physics and Chemistry*, 3rd ed. (Elsevier Science, Amsterdam, 2007).

Supplemental Materials

Linear response of stochastic reactive systems

Linear Fokker-Planck equation and its stationary distribution

In the main text, we encounter multiple times the linear stochastic differential equation (SDE) of the form

$$\frac{d\vec{y}}{dt} = \mathbf{A}\vec{y} + \vec{\eta}(t), \quad (\text{S1})$$

where \mathbf{A} is independent of \vec{y} and $\vec{\eta}$ are Gaussian white noises with zero mean and correlator

$$\langle \vec{\eta}(t) \vec{\eta}^T(t') \rangle = \mathbf{B}\delta(t - t'). \quad (\text{S2})$$

The noise matrix \mathbf{B} is symmetric (*i.e.* $\mathbf{B}^T = \mathbf{B}$) and also supposed independent of \vec{y} . Equation (S1) is tantamount to the Fokker-Planck equation for the probability density $P(\vec{y}, t)$ [24]:

$$\frac{\partial P(\vec{y}, t)}{\partial t} = - \sum_{i,j} A_{ij} \frac{\partial}{\partial y_i} (y_j P) + \frac{1}{2} \sum_{i,j} \frac{\partial^2}{\partial y_i \partial y_j} (B_{ij} P). \quad (\text{S3})$$

As shown in (*e.g.*) [25], the stationary distribution is Gaussian and takes the form

$$P_s(\vec{y}) = \frac{1}{\sqrt{\det(2\pi\Xi)}} \exp\left(-\frac{1}{2}\vec{y}^T \Xi^{-1} \vec{y}\right), \quad (\text{S4})$$

where the covariance matrix Ξ is symmetric and given by the Sylvester's equation,

$$\mathbf{A}\Xi + \Xi\mathbf{A}^T + \mathbf{B} = 0. \quad (\text{S5})$$

In two dimensions, this equation can be solved [24] leading to an explicit formula for Ξ :

$$\Xi = \frac{(\mathbf{A} - \mathbb{1}_2 \text{tr}\mathbf{A}) \mathbf{B} (\mathbb{1}_2 \text{tr}\mathbf{A} - \mathbf{A})^T - \mathbf{B} \det \mathbf{A}}{2 \text{tr}\mathbf{A} \det \mathbf{A}}. \quad (\text{S6})$$

The mean amplification factor $\langle \|\vec{y}\|^2 \rangle$

We now wish to find an expression for the mean amplification factor, $\langle \|\vec{y}\|^2 \rangle$, used in the main text to quantify the linear response of a stochastic reactive system. The norm of \vec{y} is the Euclidean norm $\|\vec{y}\| = \sqrt{\sum_i |y_i^2|}$. Specifically, we want to compute the integral:

$$\langle \|\vec{y}\|^2 \rangle = \int_{\mathbb{R}^D} d\vec{y} P_s(\vec{y}) \|\vec{y}\|^2, \quad (\text{S7})$$

where the distribution $P_s(\vec{y})$ is given by Eq. (S4). Therefore,

$$\langle \|\vec{y}\|^2 \rangle = \frac{1}{\sqrt{\det(2\pi\Xi)}} \int d\vec{y} \exp\left(-\frac{1}{2}\vec{y}^T \Xi^{-1} \vec{y}\right) \|\vec{y}\|^2. \quad (\text{S8})$$

To evaluate this integral, we use the identity

$$\int \|\vec{p}\|^2 e^{-\vec{p}^T \mathbf{M} \vec{p}} d\vec{p} = \frac{1}{2} \text{Tr}(\mathbf{M}^{-1}) \int e^{-\vec{p}^T \mathbf{M} \vec{p}} d\vec{p}, \quad (\text{S9})$$

with $\mathbf{M} = 1/2\Xi^{-1}$, which yields the compact expression:

$$\langle \|\vec{y}\|^2 \rangle = \text{Tr} \Xi \quad (\text{S10})$$

In the following, we assume for convenience that the noise matrix \mathbf{B} is a multiple of identity matrix $\mathbb{1}$ ($\mathbf{B} = \sigma^2 \mathbb{1}$), a choice that can be made without losing in generality. In fact, since \mathbf{B} is symmetric, it is diagonalized by an orthogonal matrix which one can use to transform the noises; the resulting diagonal matrix can then be mapped to the identity matrix simply by rescaling the variables \vec{y} . Now, we will write the matrix $\mathbf{\Xi}$ in terms of \mathbf{A} and what we call the Hermitianizer of \mathbf{A} , defined as

$$\mathbf{G} = -\frac{1}{2}\sigma^2 \mathbf{\Xi}^{-1} \mathbf{A}^{-1}, \quad (\text{S11})$$

which yields a symmetrization of matrix \mathbf{A} : even though \mathbf{A} is not symmetric, $\mathbf{A} \neq \mathbf{A}^T$, the product $\mathbf{GA} = -2^{-1}\sigma^2 \mathbf{\Xi}^{-1}$ is a symmetric matrix. Sylvester equation (S5) written in terms of \mathbf{G} simplifies to

$$\frac{1}{2}(\mathbf{G}^{-1} + \mathbf{G}^{-T}) = \mathbb{1}, \quad (\text{S12})$$

indicating that the hermitian part of \mathbf{G}^{-1} is identity. Alternatively, the Hermitianizer of \mathbf{A} can be defined as the unique matrix satisfying Eq. (S12) whose product with \mathbf{A} is Hermitian. Now we can write the mean squared value of the norm \vec{y} in terms of \mathbf{A} and \mathbf{G} by substituting Eq. (S11) in Eq. (S10):

$$\langle \|\vec{y}\|^2 \rangle = -\frac{1}{2}\sigma^2 \text{Tr}(\mathbf{A}^{-1} \mathbf{G}^{-1}) \quad (\text{S13})$$

When \mathbf{A} is a 2×2 matrix, the trace of the inverse can be written as trace over determinant:

$$\langle \|\vec{y}\|^2 \rangle = -\frac{1}{2}\sigma^2 \frac{\text{Tr}(\mathbf{GA})}{\det(\mathbf{G}) \det(\mathbf{A})} \quad (\text{S14})$$

$\text{Tr}(\mathbf{GA})$ can be simplified by taking the trace of Eq. (S11)

$$\text{Tr}(\mathbf{GA}) = -\frac{1}{2}\sigma^2 \text{Tr}(\mathbf{\Xi}^{-1}). \quad (\text{S15})$$

Also, by multiplying the right-hand side of the Sylvester equation (S5) by $\mathbf{\Xi}^{-1}$:

$$\mathbf{A} + \mathbf{\Xi} \mathbf{A}^T \mathbf{\Xi}^{-1} = -\sigma^2 \mathbf{\Xi}^{-1}. \quad (\text{S16})$$

and taking the trace we have (recalling that $\text{Tr}(\mathbf{\Xi} \mathbf{A}^T \mathbf{\Xi}^{-1}) = \text{Tr}(\mathbf{A}^T) = \text{Tr}(\mathbf{A})$):

$$\sigma^2 \text{Tr}(\mathbf{\Xi}^{-1}) = -2 \text{Tr}(\mathbf{A}) \quad (\text{S17})$$

From Eq. (S17) and Eq. (S15) it follows that $\text{Tr}(\mathbf{GA}) = \text{Tr}(\mathbf{A})$. which we can use to simplify Eq. (S13):

$$\langle \|\vec{y}\|^2 \rangle = -\frac{\sigma^2}{2} \frac{\text{Tr} \mathbf{A}}{\det \mathbf{G} \det \mathbf{A}} = -\frac{1}{2}\sigma^2 \det(\mathbf{G}^{-1}) \text{Tr}(\mathbf{A}^{-1}). \quad (\text{S18})$$

Non-normality for a 2×2 matrix \mathbf{A}

For a 2×2 matrix \mathbf{A} given by its elements

$$\mathbf{A} = \begin{pmatrix} a_{11} & a_{12} \\ a_{21} & a_{22} \end{pmatrix}, \quad (\text{S19})$$

we can solve for $\mathbf{\Xi}$ from Eq. (S6) and substitute in Eq. (S11) to find the matrix \mathbf{G} in terms of matrix elements of \mathbf{A} :

$$\mathbf{G} = \begin{pmatrix} \frac{(a_{11}+a_{22})^2}{(a_{12}-a_{21})^2+(a_{11}+a_{22})^2} & -\frac{(a_{12}-a_{21})(a_{11}+a_{22})}{(a_{12}-a_{21})^2+(a_{11}+a_{22})^2} \\ \frac{(a_{12}-a_{21})(a_{11}+a_{22})}{(a_{12}-a_{21})^2+(a_{11}+a_{22})^2} & \frac{(a_{11}+a_{22})^2}{(a_{12}-a_{21})^2+(a_{11}+a_{22})^2} \end{pmatrix}. \quad (\text{S20})$$

The non-normality index \mathcal{H} is given by the inverse of the determinant of \mathbf{G} :

$$\mathcal{H}(\mathbf{A}) = \det(\mathbf{G}^{-1}) = 1 + \frac{(a_{12} - a_{21})^2}{(a_{11} + a_{22})^2}. \quad (\text{S21})$$

If the eigenvalues of \mathbf{A} are real, we can rewrite this expression in terms of the eigenvalues and the angle between the eigenvectors of \mathbf{A} . Let $\Delta > 0$ be the discriminant of the characteristic polynomial of \mathbf{A} :

$$\Delta = (a_{11} - a_{22})^2 + 4 a_{12} a_{21}. \quad (\text{S22})$$

If λ_1 and λ_2 are the two eigenvalues of \mathbf{A} , and \vec{v}_1 and \vec{v}_2 are the two eigenvectors, we have

$$\begin{aligned} (\lambda_1 + \lambda_2)^2 &= (a_{11} + a_{22})^2, & (\lambda_1 - \lambda_2)^2 &= \Delta, \\ \cos^2(\theta) &= \left(\frac{\vec{v}_1 \cdot \vec{v}_2}{\|\vec{v}_1\| \|\vec{v}_2\|} \right)^2, & \cot^2(\theta) &= \frac{\cos^2(\theta)}{1 - \cos^2(\theta)} = \frac{(a_{11} - a_{22})^2}{\Delta}. \end{aligned} \quad (\text{S23})$$

Now it is clear that

$$\mathcal{H}(\mathbf{A}) = 1 + \cot^2(\theta) \left(\frac{\lambda_1 - \lambda_2}{\lambda_1 + \lambda_2} \right)^2. \quad (\text{S24})$$

Linear stochastic differential equations with complex variables

Consider a similar set of SDEs of the the form

$$\frac{d\vec{y}}{dt} = \mathbf{A}\vec{y} + \vec{\eta}(t), \quad (\text{S25})$$

where now \vec{y} and $\vec{\eta}$ are vectors with complex variables, and $\vec{\eta}$ is a Gaussian white noise with zero mean and correlator

$$\begin{aligned} \langle \vec{\eta}(t) \vec{\eta}^\dagger(t') \rangle &= \mathbf{B} \delta(t - t'), \\ \langle \vec{\eta}(t) \vec{\eta}^T(t') \rangle &= 0. \end{aligned} \quad (\text{S26})$$

where the \dagger symbol represents the transpose conjugate. The analysis in the previous section can be generalized by evaluating the expected value of $\vec{y}(t) \vec{y}^\dagger(\tau)$ and $\vec{y}(t) \vec{y}^T(\tau)$ at steady state for $t = \tau$ to obtain the following relationships for the *covariance* and *relation* matrices

$$\begin{aligned} \mathbf{A} \langle \vec{y} \vec{y}^\dagger \rangle + \langle \vec{y} \vec{y}^\dagger \rangle \mathbf{A}^\dagger + \mathbf{B} &= 0 \\ \mathbf{A} \langle \vec{y} \vec{y}^T \rangle + \langle \vec{y} \vec{y}^T \rangle \mathbf{A}^T &= 0 \end{aligned} \quad (\text{S27})$$

The first equation is the analogue of equation of Sylvester Eq. (S5) for the Hermitian covariance matrix $\Xi = \langle \vec{y} \vec{y}^\dagger \rangle$, while the second equation implies that the symmetric relation matrix $\mathbf{C} = \langle \vec{y} \vec{y}^T \rangle$ is equal to zero. Therefore, at steady state, \vec{y} obeys a circularly symmetric complex Gaussian distribution of the form

$$P_s(\vec{y}) = \frac{1}{\det(2\pi\Xi)} \exp\left(-\frac{1}{2} \vec{y}^\dagger \Xi^{-1} \vec{y}\right). \quad (\text{S28})$$

Notice the different normalization factor compared to Eq (S4), as it is normalized over \mathbb{C}^D instead of \mathbb{R}^D .

To compute the mean square value of the norm of \vec{y} , we can follow similar analysis to that of section . Here, we highlight the differences. The mean square norm is define as

$$\langle \|\vec{y}\|^2 \rangle = \int_{\mathbb{C}^D} d\vec{y} P_s(\vec{y}) \|\vec{y}\|^2, \quad (\text{S29})$$

with the norm $\|\vec{y}\| = \sqrt{\vec{y}^\dagger \vec{y}}$. The complex version of Eq. (S9) can be evaluated by diagonalizing the matrix \mathbf{M} and write the integral on a $2D$ -dimensional real space. The result is given by

$$\int_{\mathbb{C}^D} \|\vec{p}\|^2 e^{-\vec{p}^\dagger \mathbf{M} \vec{p}} d\vec{p} = \text{Tr}(\mathbf{M}^{-1}) \int_{\mathbb{C}^D} e^{-\vec{p}^\dagger \mathbf{M} \vec{p}} d\vec{p}, \quad (\text{S30})$$

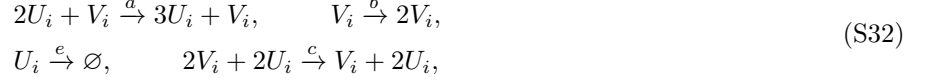
where the factor $1/2$ is canceled by the fact that each eigenvalue of \mathbf{M}^{-1} should be counted twice in the $2D$ -dimensional space, once for the real part and once for the imaginary part. As a result, there will be an extra factor 2 in Eq. (S10), Eq. (S13), and Eq. (S18). In particular ,

$$\langle \|\vec{y}\|^2 \rangle = -\sigma^2 \text{Tr}(\mathbf{A}^{-1} \mathbf{G}^{-1}) \quad (\text{S31})$$

Analysis of model by Ridolfi et al.

From individual level model to SDEs

In this section we derive a the stochastic extension of the model by Ridolfi et al. [15] by expanding the master equation corresponding to the individual level model defined by the following set of reactions



where U_i and V_i are the species U and V in the site i , and the diffusion reactions



where $\langle i \rangle$ is the set of sites neighboring i , $\delta_u = D_U/\Omega^{2/D}$, $\delta_v = D_V/\Omega^{2/D}$, D_U and D_V are the diffusion constants, and Ω is the volume of each site. The state of the system is specified by the concentration vectors $\vec{q}_i \equiv (u_i, v_i) \equiv (U_i, V_i)/\Omega$.

Each reaction of reaction scheme (S33) takes the system from a state $\{\vec{q}_i\}$ to $\{\vec{q}'_i\}$ with probability per unit time $T(\{\vec{q}'_i\}|\{\vec{q}_i\})$. These transition rates are given from the law of mass action:

$$\begin{aligned} T(\vec{q}_i + \vec{s}_1 | \vec{q}_i) &= \Omega a u_i^2 v_i, & T(\vec{q}_i + \vec{s}_2 | \vec{q}_i) &= \Omega b v_i, \\ T(\vec{q}_i - \vec{s}_1 | \vec{q}_i) &= \Omega e u_i, & T(\vec{q}_i - \vec{s}_2 | \vec{q}_i) &= \Omega c u_i^2 v_i^2, \end{aligned} \quad (\text{S34})$$

and for every $j \in \langle i \rangle$

$$\begin{aligned} T(\vec{q}_i - \vec{s}_1, \vec{q}_j + \vec{s}_1 | \vec{q}_i, \vec{q}_j) &= \Omega \delta_u u_i, \\ T(\vec{q}_i - \vec{s}_2, \vec{q}_j + \vec{s}_2 | \vec{q}_i, \vec{q}_j) &= \Omega \delta_v v_i, \end{aligned} \quad (\text{S35})$$

where

$$\vec{s}_1 = \Omega^{-1} \begin{pmatrix} 1 \\ 0 \end{pmatrix}, \quad \vec{s}_2 = \Omega^{-1} \begin{pmatrix} 0 \\ 1 \end{pmatrix}. \quad (\text{S36})$$

The master equation for the time evolution of the probability of finding the system at a state $\{\vec{q}_i\}$, $P(\{\vec{q}_i\}, t)$ can be written as

$$\frac{dP(\{\vec{q}_i\}, t)}{dt} = \sum_{\{\vec{q}'_i\}} (T(\{\vec{q}_i\}|\{\vec{q}'_i\}) - T(\{\vec{q}'_i\}|\{\vec{q}_i\})) \quad (\text{S37})$$

Following [22], we can expand the right hand side of Eq. (S37) to second order in Ω^{-1} obtaining a Fokker-Planck equation corresponding the following set of stochastic differential equations

$$\begin{aligned} \frac{du_i}{dt} &= u_i(a u_i v_i - e) + \delta_u \sum_{j \in \langle i \rangle} (u_j - u_i) + \xi_i(t), \\ \frac{dv_i}{dt} &= v_i(b - c u_i^2 v_i) + \delta_v \sum_{j \in \langle i \rangle} (v_j - v_i) + \eta_i(t), \end{aligned} \quad (\text{S38})$$

where ξ_i 's and η_i 's are zero mean Gaussian noise with correlations

$$\begin{aligned} \langle \xi_i(t) \xi_j(t') \rangle &= \frac{\delta(t-t')}{\Omega} \left(\left(u_i(a u_i v_i + e) + \delta_u \sum_{k \in \langle i \rangle} (u_i + u_k) \right) \delta_{i,j} - \delta_u (u_i + u_j) \chi_{\langle i \rangle}(j) \right) \\ \langle \eta_i(t) \eta_j(t') \rangle &= \frac{\delta(t-t')}{\Omega} \left(\left(v_i(b + c u_i^2 v_i) + \delta_v \sum_{k \in \langle i \rangle} (v_i + v_k) \right) \delta_{i,j} - \delta_v (v_i + v_j) \chi_{\langle i \rangle}(j) \right) \end{aligned} \quad (\text{S39})$$

and the characteristic function, $\chi_{\langle i \rangle}$, of $\langle i \rangle$ is defined as

$$\chi_{\langle i \rangle}(j) = \begin{cases} 1 & j \in \langle i \rangle \\ 0 & j \notin \langle i \rangle \end{cases}. \quad (\text{S40})$$

By defining $\vec{f}(\vec{q}) \equiv (f, g) \equiv (u(auv - e), v(b - cu^2v))$, $\vec{\xi}_i \equiv (\xi_i, \eta_i)$, $\delta \equiv \text{diag}(\delta_u, \delta_v)$, and $(\Delta\vec{q})_i \equiv \sum_{j \in \langle i \rangle} (\vec{q}_j - \vec{q}_i)$, Eq. (S38) can be written in the simple form

$$\frac{d\vec{q}_i}{dt} = \vec{f}(\vec{q}_i) + \delta (\Delta\vec{q})_i + \vec{\xi}_i(t). \quad (\text{S41})$$

Equation (S41) is the discrete space version of Eq. (8) of the main text. Continuous limit can be taken at any point in the following analysis to recover the continuous space stochastic partial differential equations of type analyzed in the main text. We continue with the discrete version where the analytic results can be more readily compared to the simulation.

The deterministic part of our model has a fixed point $\vec{q}^* \equiv (u^*, v^*) = (ba/ce, e^2c/a^2b)$, obtained by setting $\vec{f}(\vec{q})$ equal to zero. We can linearize Eq. (S41) around the fixed point \vec{q}^* , by defining $\vec{p}_i \equiv ((u_i - u^*)/\sqrt{2u^*e}, (v_i - v^*)/\sqrt{2v^*b})$ which are the rescaled deviations of \vec{q}_i from \vec{q}^* ,

$$\frac{d\vec{p}_i}{dt} = \mathbf{J}\vec{p}_i + \delta(\Delta\vec{p})_i + \vec{\xi}_i(t), \quad (\text{S42})$$

where the linear stability operator \mathbf{J} is defined as the Jacobian of the transformed function f at the fixed point $\vec{p} = 0$ is given by

$$\mathbf{J} = \begin{pmatrix} e & b^{\frac{3}{2}}a^{\frac{3}{2}} \\ -\frac{2e^2c}{a^{\frac{3}{2}}b^{\frac{1}{2}}} & -b \end{pmatrix} \quad (\text{S43})$$

Evaluating Eq. (S39) at \vec{q}^*

$$\begin{aligned} \langle \xi_i(t) \xi_j(t') \rangle &= \frac{\delta(t-t')}{\Omega} \left((1 + \delta_u n/e) \delta_{i,j} - \delta_u \chi_{\langle i \rangle}(j) \right), \\ \langle \eta_i(t) \eta_j(t') \rangle &= \frac{\delta(t-t')}{\Omega} \left((1 + \delta_v n/b) \delta_{i,j} - \delta_v \chi_{\langle i \rangle}(j) \right), \end{aligned} \quad (\text{S44})$$

where $n \equiv |\langle i \rangle|$ is the number of neighbors of each site. Note that for $b > e$, both of the eigenvalues of \mathbf{J} have negative real parts, making \vec{q}^* an attractor of the dynamics in the absence of the diffusion.

To examine the spatial stability of \vec{q}^* , we need to diagonalize the discrete Laplacian operator Δ , by defining the discrete Fourier transform of a sequence $\{s_{\vec{n}}\}$ as

$$\tilde{s}_{\vec{k}} \equiv (\mathcal{F}[\{s_{\vec{n}}\}])_{\vec{k}} \equiv \frac{1}{\sqrt{N^D}} \sum_{\vec{n}} e^{-2\pi i \vec{k} \cdot \vec{n} / N} s_{\vec{n}}. \quad (\text{S45})$$

We drop the tildes on the Fourier variable with the convention that the variables with index k are Fourier variables. Equation (S42) under this transformation becomes

$$\frac{d\vec{p}_{\vec{k}}}{dt} = \mathbf{K}\vec{p}_{\vec{k}} + \vec{\xi}_{\vec{k}}(t), \quad \mathbf{K} = \mathbf{J} + \Delta(\vec{k})\delta, \quad (\text{S46})$$

where $\Delta(\vec{k})$ is the discrete Fourier transform of the discrete Laplacian operator given by

$$\Delta(\vec{k}) \equiv -2 \sum_{l=1}^D (1 - \cos(2\pi k_l / N)) \quad (\text{S47})$$

and

$$\begin{aligned} \langle \xi_{\vec{k}}(t) \xi_{\vec{k}'}^*(t') \rangle &= \Omega^{-1} \left(1 - e^{-1} \delta_u \Delta(\vec{k}) \right) \delta_{\vec{k}, \vec{k}'} \delta(t-t'), \\ \langle \eta_{\vec{k}}(t) \eta_{\vec{k}'}^*(t') \rangle &= \Omega^{-1} \left(1 - b^{-1} \delta_v \Delta(\vec{k}) \right) \delta_{\vec{k}, \vec{k}'} \delta(t-t'). \end{aligned} \quad (\text{S48})$$

For the regime that we observe stochastic patterns, the contribution of the diffusion process in the amplitude of the noise in Eq. (S48) is very small and will be neglected for simplicity. This approximation is not necessary, since there is always a change of variables that simplifies the correlation matrix to a multiple of the identity matrix (this is the reason for the rescaling in the definition of \vec{p}). With this approximation

$$\left\langle \vec{\xi}_{\vec{k}}(t) \vec{\xi}_{\vec{k}'}^{\dagger}(t') \right\rangle = \Omega^{-1} \delta_{\vec{k}, \vec{k}'} \delta(t-t') \mathbf{1} \quad (\text{S49})$$

where $\vec{\xi}_{\vec{k}'}^{\dagger}$ is the conjugate transpose of $\vec{\xi}_{\vec{k}}$, and $\mathbf{1}$ is the 2×2 identity matrix.

Phase diagram of pattern formation

The pattern forming behavior of the model defined by (S33) can be understood by analyzing the eigenvalues of \mathbf{K} as a function of \vec{k} . Matrix \mathbf{K} can be written in elements from Eq. (S46) and Eq. (S43):

$$\mathbf{K} = \begin{pmatrix} e + \Delta(\vec{k})\delta_u & \frac{b^{\frac{3}{2}}a^{\frac{3}{2}}}{ce} \\ -\frac{2e^2c}{a^{\frac{3}{2}}b^{\frac{1}{2}}} & -b + \Delta(\vec{k})\delta_v \end{pmatrix} \quad (\text{S50})$$

As it will become clear, most of the properties of the system depend on the following three parameters

$$\rho = \frac{b}{e}, \quad \nu = \frac{ec}{a^{\frac{3}{2}}b^{\frac{1}{2}}}, \quad r = \frac{\delta_v}{\delta_u} = \frac{D_V}{D_U} \quad (\text{S51})$$

in the following analysis, we will write various expression in terms of these parameters, wherever we can. We start with \mathbf{K}

$$\mathbf{K} = \begin{pmatrix} e + \Delta(\vec{k})\delta_u & b/\nu \\ -2e\nu & -b + \Delta(\vec{k})\delta_v \end{pmatrix} \quad (\text{S52})$$

The largest eigenvalue of \mathbf{K} is given by

$$\lambda(\vec{k}) = \frac{1}{2} \left(\sqrt{b^2 - 2b\Delta(\vec{k})(\delta_v - \delta_u) - 6be + (e - \Delta(\vec{k})(\delta_v - \delta_u))^2} - b + \Delta(\vec{k})(\delta_v + \delta_u) - e \right). \quad (\text{S53})$$

Notice that the eigenvalues of \mathbf{K} are independent of ν . For small \vec{k} , $\Delta(\vec{k})$ is a monotonically decreasing function of \vec{k} (proportional to $-k^2$). We define $y = -\Delta(\vec{k})$. To determine if λ monotonically decays or if it has a maximum at some $\vec{k}_0 \neq 0$, we can differentiate λ with respect to y and see if it has a positive root. The largest root of $\frac{d\lambda}{dy}$ is given by

$$y_0 = -\Delta(\vec{k}_0) = \frac{(r+1)\sqrt{2ber} - br - er}{\delta_u(r-1)r}. \quad (\text{S54})$$

For y_0 to be greater than zero we need

$$\rho < \frac{(1+r+r^2+(r+1)\sqrt{r^2+1})}{r}. \quad (\text{S55})$$

We can find the condition on the ratio of the diffusion constants by inverting this inequality:

$$r > \frac{1-2\rho+\rho^2+(1+\rho)\sqrt{1+\rho(\rho-6)}}{4\rho} = f_1(\rho). \quad (\text{S56})$$

The condition for formation of stochastic pattern is $\lambda(\vec{k}_0) > \Re(\lambda(0))$. We can find $\lambda(\vec{k}_0)$ and $\lambda(0)$ by substituting $y_0 = y(\vec{k}_0)$ from Eq. (S54) and $y(0) = 0$ in Eq. (S53):

$$\lambda(\vec{k}_0) = \frac{b+er-\sqrt{8ber}}{r-1}, \quad \lambda(0) = \frac{1}{2} \left(\sqrt{b^2-6be+e^2} - b + e \right). \quad (\text{S57})$$

Then, $\lambda(\vec{k}_0) > \Re(\lambda(0))$ simplifies to

$$r > \frac{-1+14\rho-\rho^2+4\sqrt{-2\rho(1+\rho(\rho-6))}}{(1+\rho)^2} = f_2(\rho). \quad (\text{S58})$$

Condition for deterministic Turing pattern is a lot simpler; we just need $\lambda(\vec{k}_0) > 0$ which simplifies to

$$r > (3+2\sqrt{2})\rho = f_3(\rho). \quad (\text{S59})$$

When r is greater than $f_1(\rho)$ and $f_2(\rho)$ but less than $f_3(\rho)$, the system exhibits stochastic patterns (blue region in Fig. 3 of the main text), while we observe the deterministic patterns when r is greater than f_3 (orange region of Fig. 3 of the main text).

Non-normality of the model

The amplification of our stochastic patterns depend on the non-normality index of $\mathbf{K}_0 = \mathbf{K}(\vec{k}_0)$ given by

$$\mathbf{K}_0 = \begin{pmatrix} e - y_0 \delta_u & b/\nu \\ -2e\nu & -b - y_0 \delta_v \end{pmatrix}, \quad (\text{S60})$$

where $y_0 = -\Delta(\vec{k}_0)$. We use Eq. (S21) to calculate the non-normality index of \mathbf{K}_0 :

$$\mathcal{H}(\mathbf{K}_0) = 1 + \left(\frac{b + 2e\nu^2}{\nu(b - e + y_0(\delta_u + \delta_v))} \right)^2. \quad (\text{S61})$$

We substitute y_0 from Eq. (S54) and rewrite the resulting expression in terms of ρ , r , and ν :

$$\mathcal{H}(\mathbf{K}_0) = 1 + \left(\frac{2\nu^2 + \rho}{\nu \left(\rho - 1 + \frac{(r+1)(-\rho r + (r+1)\sqrt{2\rho r - r})}{(r-1)r} \right)} \right)^2 \quad (\text{S62})$$

Since the eigenvalues of \mathbf{K} do not depend on ν , one can change $\mathcal{H}(\mathbf{K}_0)$ by changing ν without moving the system in its phase diagram (see Fig. 3 of the main text). This can be done by changing the ratio of $a/c^{2/3}$ without affecting ρ .